

Removal of copper (II) from aqueous solution using granular sodium alginate/activated carbon hydrogel in a fixed-bed column

Leila Adhami^a, Masoomeh Mirzaei^{b,*}

^aDepartment of Chemical Engineering, Omidyeh branch, Islamic Azad University, Omidyeh, Iran, Tel. +989163502263, email: leila.adhami71@gmail.com, Tel. +989177713599, email: mostafa.narimani@gmail.com

^bDepartment of Chemical Engineering, Mahshahr branch, Islamic Azad University, Mahshahr, Iran, Tel. +989127057112, email: mirzaei_fateme@yahoo.com

Received 13 April 2017; Accepted 26 January 2018

ABSTRACT

Sodium alginate is a natural polysaccharide-based polymer and due to its anionic nature is effective for the adsorption heavy metals. In this study, the removal of Cu(II) ions from aqueous solutions was investigated using synthetic hydrogel of SA/AC/HA prepared by sol-gel method, and properties of composite were characterized using Fourier transform infrared spectroscopy (FTIR). The effect of various experimental conditions such as column height (3.5–4.5 cm), flow rate (6, 8, 10 ml/min) and inlet copper concentration (300, 400, 500 mg/L) on the column was studied. The experimental data were investigated by the Adam-Boohart and the Thomas and Yoon-Nelsone kinetic models. The experimental and theoretical adsorption capacity of column (q_e) (calculated by Thoms model) were proportional error = $\pm 0.308\%$. Adsorbent has regeneration ability using 4% HCl, for recovery up to 5 times, with percentage coefficient (D%) between 70–82.75%.

Keywords: Sodium alginate; Copper ion(II); Fixed-bed column; Adsorption; Kinetic model

1. Introduction

With the rapid development of industry, the heavy metals release rate is increasing in surface waters [1]. Water pollution by heavy metals due to toxic effects on human life and other living microorganisms has become a serious problem [2]. Heavy metals may cause various diseases, such as cancer, tumors, heart defects and mutations [3]. Heavy metals such as lead, mercury, copper, cadmium, zinc, nickel and chromium are non-environmentally friendly and they are toxic in low concentration [4]. Copper as one of the common heavy metals has been widely used for many industrial productions; the large amount of copper-based wastes using different processes can be released into water [5]. For example, the wastewater from the metal finishing industry (e-coating process) can contain 20 ppm each of nickel and zinc. On the other hand, the allowable concentration of Zn^{2+} and Ni^{2+} is 2 ppm [6]. Wastewaters and heavy metals exist in

many industries, such as metal plating, mining operations, the color of the textile industry [4], printing, papermaking, food coloring [7], leather, rubber, plastics [8], battery making [9], and urban traffic [10].

Methods are commonly used for the removal of heavy metals from water are sedimentation, adsorption, ion exchange, reverse osmosis, electrochemical recovery, and hyper filtration, membrane separation, evaporation, coagulation, flotation, oxidation and biological adsorption [11]. The use of these methods has some limitations like cost, complexity, efficiency or secondary scraps [12].

Hydrogels consist of three-dimensional polymer networks which are used in sensors, separation membranes, adsorbents and they are most useful in pharmaceuticals as drug delivery systems to solve some environmental and biological problems as well as modern technology [13].

Super adsorbent polymer has a highly hydrophilic polymer network which due to their three-dimensional cross-

*Corresponding author.

linking are able to swell. Also they can capture and store water up to 100 times more than their own weight [14]. This polymer has high capacity and the inflation speed as well as optimal gel texture [15]. Modern industries are created the interest to natural polymers rather than synthetic ones. Natural polymers include starch, cellulose, chitosan, collagen, crack and alginate [16].

Alginate is a naturally occurring anionic polymer typically obtained from brown seaweed, and has been extensively investigated and used for many biomedical applications, due to its biocompatibility, low toxicity, relatively low cost, and mild gelation by addition of divalent cations such as Ca^{2+} [17]. This natural polymer is an anionic copolymer composite containing β -D-mannuronic acid and α -L-guluronic acid that is linked by 1-4 glycosidic chains. Polysaccharide gel is derived mainly from displacement of Na^+ ion deposits in α -L-guluronic acid (G) residues with bivalent cations [18]. Activated carbon is one of the oldest and most widely used of adsorbents to remove and restore organic and inorganic contaminations from waters and wastewaters. The use of activated carbon in adsorption process is mainly depends on surface chemistry and the pore structure of the porous carbons [19].

There are many results reporting the removal of heavy metals from aqueous solution using a wide range of adsorbents, the removal of nickel from water were done by using nano-crystalline calcium hydroxyapatite adsorbent [6]. Composite adsorbents were synthesized from activated carbon and silica-gel via the sol-gel and drying processes in limited pressure to remove their cadmium [20]. The removal of Cadmium(II) from water using sunflower waste carbon calcium–alginate beads (SWC-CAB) in continuous flow fixed bed column is reported [21]. A down flow fixed bed column study was performed using sunflower stem carbon–calcium alginate beads (SSC-CAB) for the adsorptive removal of Cr(VI) at various bed heights, initial Cr(VI) concentrations, and flow rates at preoptimized pH = 2.0 [22].

A study reported the assessment of helical coil-packed bed columns for Zn^{2+} adsorption breakthrough curves with different characteristics and a comparison has been performed with regard to the results of straight fixed-bed columns [23]. In a study, activated carbon was produced from oil palm shell by two-step chemical activation using K_2CO_3 as the chemical activant in the ratio 1:2 for the removal of phenol in a fixed-bed column. The study of several factors including bed depth, initial phenol concentration, and flow rate were conducted. Breakthrough curve models indicated that Yoon–Nelson model gave better fit to the experimental data than both the Adam–Bohart and Thomas models [24]. Nanocomposites were synthesized by porous granules of double reticular graphene/alginate and the potential removal of blue methylene from waters was investigated in both batch and continuous experiments for this adsorbent [25].

In this study, the removal of Cu(II) from aqueous solutions was carried out using synthetic hydrogel of sodium alginate/active carbon/hydroxyapatite prepared in a fixed-bed column. In addition, we examined the effects of various experimental conditions such as column depth, flow rate and inlet copper concentration and kinetic models were employed to describe the adsorption process.

2. Experimental study

2.1. Materials

Sodium alginate, Hydroxyapatite [$\text{Ca}_5(\text{OH})(\text{PO}_4)_3$] were purchased from Sigma-Aldrich Co. USA, Commercial activated carbon of coconut, Copper(II) sulfate pentahydrate ($\text{CuSO}_4 \cdot 5\text{H}_2\text{O}$), Ammonia (NH_3), Calcium chloride ($\text{CaCl}_2 \cdot 2\text{H}_2\text{O}$), Hydrochloric acid (HCl, 37%), were purchased from Merck Co. All solutions were prepared by distilled water.

2.2. Methods

2.2.1. Adsorbent synthesis

To prepare adsorbent synthesis, firstly 0.8 g of hydroxyapatite is added to distilled water and then, the mixture placed in an ultrasonic bath (BANDELIN Electronic GmbH & Co, Germany) for 15 min to obtain distribution of hydroxyapatite (HA) particles. When a homogenous solution resulted, it placed under conditions with magnetic stirrer (IKA Co, RH b2, Germany). In this phase, 6 g of sodium alginate is added slowly and in a step-by-step manner to the mixture under agitating s, Finally, 1 g activated carbon is added to the gel-type mixture. As soon as sodium alginate is added to solution, the solution is transferred slowly to the gel-type mixture to obtain a homogenous gel, then the mixture is placed under agitating.

After the injection of the gel into the salty solution, the injected spherical gels are placed in the salty solution to achieve their stable form, then, the spherical gels need to be washed with distilled water to remove salt from their surface. The spherical gels are placed on the plate to get exhausted by water and dried. Granules are observed with size ranges 1–1.5 mm after drying (Fig. 1).

2.2.2. Data analysis of fixed-bed column

To carry out adsorbance experiments, a glass tube ($d = 1.5$ and $h = 30$ cm) was used as the column. Plastic valves at top and bottom of column were used to control input/output flow rate, and column opened from both sides, and also closed its entrance/exit, in addition, a cap has been used. The pollutant solution in a reservoir has been placed at the top of column that reservoir' exit flow rate was controlled by a valve.

Ceramic filler was placed at the bottom of column and between granules to prevent packing and movement of hydrogel particles. Before launching any test, water flow was passed through the column to remove impurities.

Then, the solution kept in the tank was flowed from top of the column and the discharge rate was controlled by outlet valve. The output solutions of the column were collected from lower output valve from beginning to end the process. Output copper concentration was performed by spectrophotometric analysis (UNICO 2100 SUV-Vis, New Jersey) at wavelength 615 nm. Breakthrough curve (i.e. C_t/C_0 Vs t) was drawn for all concentrations between the time and C_t/C_0 (i.e. C_t = concentration of output copper and C_0 = initial concentration of copper). All experiments were conducted at room temperature 25°C (± 3). A schematic diagram of fixed bed column adsorption by using SACH as adsorbent

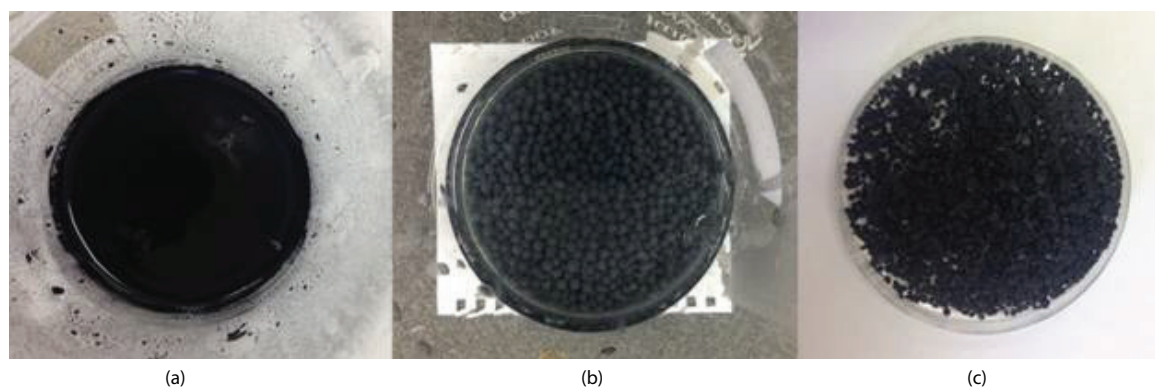


Fig. 1. Hydrogel images during the synthesis steps (a) prepared gel, (b) granules injected in salt solution, (c) dried hydrogel granules.

is shown in. To determine the maximum adsorption capacity of hydrogel granules and other parameters of the fixed bed column adsorption, Eq. (1) is proposed.

The treated effluent volume V_t (ml) can be described by the following formula:

$$V_t = Q * t_{total} \quad (1)$$

where Q is the term volumetric flow rate (ml/min) and t_{total} is the term total flow time (min) [28,30].

To calculate certain concentration and flow rate, the maximum adsorption capacity of the column q_{total} (mg) can be obtained by the upper side of the curve. The area under the adsorption capacity vs. time curve showed most adsorbed concentration of the column which can be calculated by integrating the adsorbed concentration (C_{ad} ; mg/l) vs. t (min) through the following equation:

$$q_{total} = \frac{Q}{1000} \int_{t=0}^{t=t_e} C_{ad}.dt \quad (2)$$

where C_{ad} in Eq. (2) can be obtained from the difference between input and output pollutant concentrations in accordance with Eq. (3):

$$C_{ad} = C_0 - C_t \quad (3)$$

where C_{ad} , C_0 , C_t , t_{total} and Q are the adsorbed metal concentration (mg/L), metal input concentration (mg/L), output column concentration (mg / L), total flow time (min) and volumetric flow rate (L/min), respectively.

q_e (mg/g) is equilibrium adsorption capacity of the hydrogel granules as expressed by Eq. (4) total gram of adsorbed ions (q_{total}) per grams of sorbent at the end of the adsorption time.

$$q_e = \frac{q_{total}}{m} \quad (4)$$

where m (g) is the amount of adsorbent at the column.

The total amount of pollutants entering the column W_{total} (mg) can be calculated by the following equation.

$$W_{total} = \frac{C_0 Q t_{total}}{1000} \quad (5)$$

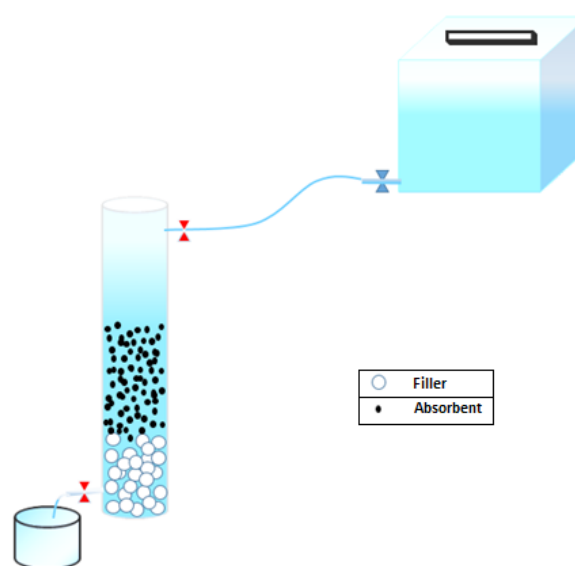


Fig. 2. To determine the maximum adsorption capacity of hydrogel granules and other parameters of the fixed bed column adsorption, Eq. (1) is proposed.

The total amount of Cu removed for R using the current column can be calculated in percentage using the following equation [30]:

$$R\% = \frac{q_{total}}{W_{total}} * 100 \quad (6)$$

2.3. Regeneration of adsorbent

To regenerate the adsorbent, a 4% hydrochloric acid solution has been used for removal of pollutants from the adsorbent. Then, the regenerated adsorbent was washed with distilled water several times (to be sure of this, whether any of acid exist in adsorbent) to be able use it to conduct further experiments [29]. Adsorbent recovery has been performed up to 5 cycles to reuse it. Re-adsorption of the adsorbent is used to study the adsorbent revival efficiency, the percent coefficient of adsorbent exclusion as well as the

percentage of adsorption in different cycles. The equation of desorption coefficient is as follow:

$$D\% = \frac{\text{mg of heavy metals which is excluded by hydrochloric acid}}{\text{mg of adsorbed metal ions on adsorbent}} * 100 \quad (7)$$

3. Results and discussion

3.1. Characterization of adsorbent

Characterization of hydrogel is very important for adsorption, hence the Fourier Transform Infrared (FTIR) Spectroscopy (Perkin Elmer, Spectrum RXI with the wavelength in the range 4000–400 cm^{-1} , USA) permits identification of the adsorbent to confirm the chemical structure of the hydrogel.

Fig 3a and 3b show FTIR spectra of sodium alginate and composite hydrogel, where the 3448.25 cm^{-1} is related to the hydroxyl groups (–OH), 1651.68–1654.05 cm^{-1} associated with symmetric vibrations of the C=O bond in carboxyl, the observed shift in absorbance of alkoxy groups from wave number 1125 cm^{-1} to 1110 cm^{-1} can be attributed to gel structure formation due to the introduction of sodium alginate.

3.2. Fixed-bed column experiments

3.2.1. Effect of bed height

To investigate the effect of column height, two different heights of about 3.5 and 4.5 cm containing 2.5 and 3.5 g adsorbent were used, respectively. In such a way, the inlet concentration was set at 500 ppm and flow rate at 6 ml/min. The effect of different bed heights on breakthrough curves obtained for Cu(II) adsorption shown in Fig. 4.

As can be seen in Fig. 4, increasing the height causes an increase in flow rate and flow time (t_{total}) between Cu(II) ions and adsorbent. If the height increased, the slope of breakthrough curve could decreased slightly, this is most likely due to an increase in sites of adsorbent for adsorbent

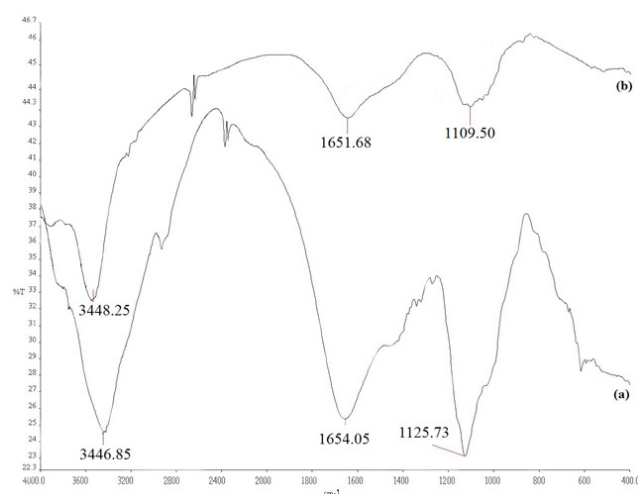


Fig. 3. FTIR spectra of: (a) sodium alginate and (b) composite hydrogel.

[21,28]. In addition, by increasing the height from 3.5 to 4.5 cm, the removal percentage was increased from 22.141% to 25.805%, so the amount of treated pollutant was also increased due to the increase in the number of the adsorbent sites, and hence, the adsorbance ability of adsorbent was increased, as shown in Table 1.

3.2.2. Effect of flow rate

The entrance flow rate is another effective parameter on the column. To investigate the effect of this parameter on the column, three different flow rates (6, 8 and 10 ml/min) have been considered. In order to study the effect of flow rate, inlet copper concentration and adsorbent column height were adjusted to 500 ppm and 35 cm, respectively. As shown in Fig. 5, the discharge adsorbent has effect on the output concentration.

As seen in Fig. 5, increasing the flow rate causes a decrease in the column effective time from 210 to 170 min and then reaches 140 min, so the breakthrough curve was also reached faster. In addition, the removal percentage obtained for Cu(II) ions was decreased from 22.141% to 17.955 due to the increase in inlet flow rate. If there was not enough time to adsorb Cu(II) ions into the hydrogel, an early breakthrough and the output time occurred at a higher flow rate, as shown in Table 1 [21,28].

3.2.3. Effect of initial concentration

To investigate the inlet concentration of pollutant in the column, it has been used from three different concentrations (300, 400 and 500 ppm), and the flow rate and the column height was adjusted to 6 ml/min and 3.5 cm, respectively. The diffusion curve is illustrated in Fig. 6. Breakthrough curves obtained for Cu(II) adsorption onto SACH at 500,400 and 300 ppm, bed depth 3.5 cm and flow rate 6 ml/min..

It is obvious that with increasing inlet concentration in the column, time over diffusion curve and the time of output column decreased, and hence the amount of pollutant removed from column increased. The removal percent of copper has been increased 22.141%, 29.929% and 32.680%, respectively for the concentrations 500, 400 and 300 ppm, Because high inlet concentration resulted in the faster sat-

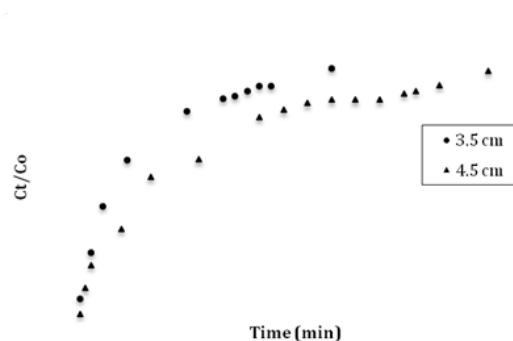


Fig. 4. Breakthrough curves obtained for Cu(II) adsorption onto SACH at two heights of 3.5 and 4.5 cm in flow rate 6 ml/min and the inlet concentration of 500 ppm.

Table 1
Experimental data and parameters obtained with different operating conditions

Z (Cm)	Q (ml/min)	C ₀ (mg/l)	t _{total} (min)	V _t (ml)	W _{total} (mg)	q _{total} (mg)	q _e (mg/g)	R%
3.5	6	500	210	1260	633	140.154	56.061	22.141
4.5	6	500	340	1440	1020	263.214	75.204	25.805
3.5	8	500	170	1360	680	136.66	54.664	20.097
3.5	10	500	140	1400	700	125.687	50.275	17.955
3.5	6	400	250	1500	600	179.574	71.829	29.929
3.5	6	300	320	1920	576	188.239	75.295	32.680

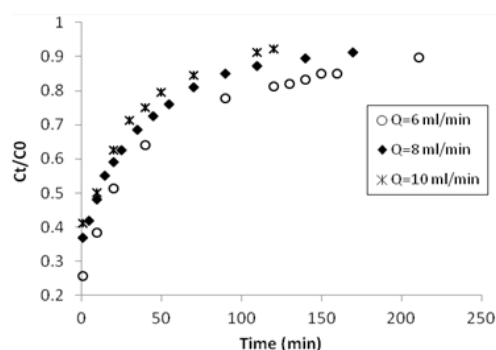


Fig. 5. Breakthrough curves obtained for Cu(II) adsorption onto SACH at three flow rates of 10, 8, 6 ml/min, bed depth 3.5 cm and inlet metal concentration 500 ppm.

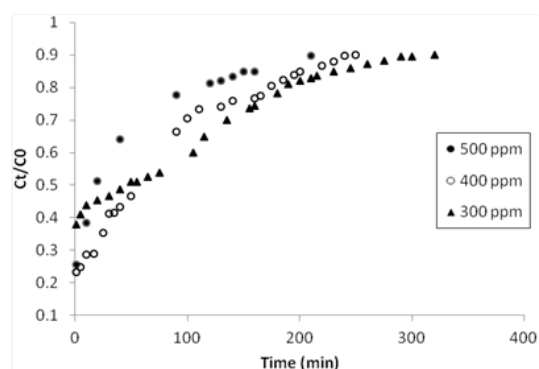


Fig. 6. Breakthrough curves obtained for Cu(II) adsorption onto SACH at 500, 400 and 300 ppm, bed depth 3.5 cm and flow rate 6 ml/min.

uration of adsorbent, diffusion curve was obtained before using all active sites of adsorbent. As can be seen in Table 1, the results showed that the adsorbent acts better in the low concentration of the heavy metal [21,28].

3.4. Kinetic investigation of column

The breakthrough models can be taken into account to predict the concentration-time profiles in order to have a better design for the adsorption process. The Thomas, Adam-Bohart and Yoon-Nelson models were applied to

predict breakthrough curves of adsorption, because these models are the most common for adsorption.

3.4.1. Adam-Bohart model

The Adam-Bohart model is one of the kinetic models that is commonly used in fixed bed adsorption. It indicates that the balance is not momentary and is appropriate for the fraction of adsorption capacity [29]. Adam-Bohart has been proposed a model based on the surface reaction theory, thus it can be assumed the adsorption rate as a function of both the residual capacity of the adsorbent and the adsorbate species concentration. This model is used for the description of the initial part of the breakthrough curve [28].

$$\ln\left(\frac{C_t}{C_0}\right) = k_{AB}C_0t - k_{AB}N_0\left(\frac{Z}{F}\right) \quad (8)$$

where k_{AB} (L/mg min) and N_0 (mg/L) are constant ratio of adsorption and saturated concentration; Z (cm) is the column length, apparent speed and F are Q ratio (cm³/min) to the cross-sectional area of column (cm²), respectively. Two parameters $k_{AB}C_0$ and $k_{AB}N_0$ (Z/F), slope and intercept, indicated the linear curve of $\ln(C_t/C_0)$ vs. time [29].

The obtained values of k_{AB} and N_0 for the column are presented in Table 2. Constant amounts in models of Adams-Bohart, Thomas and Yoon-Nelson in different operational conditions, with the linear regression analysis. With the Adam-Bohart model, the values of k_{AB} increased as the column height increased. With this enhancement, flow rate was first reduced and then increased, that with increasing in flow rate, the inlet concentration decreased. N_0 is increased as the height increased. According to this increase, the input current decreased and input metal concentration was firstly reduced and then increased. In the Adam-Bohart model, mean square error was $R^2_{avg} = 0.811$ that did not fit the experimental data well.

3.4.2. Thomas model

The Thomas model is one of the most common and widely used models in column performance theory. This model was built on the assumption that the flow in the column bed can be treated as plug flow behavior [28]. This model is represented below the plug fluid behavior in the bed.

$$\ln\left(\frac{C_0}{C_t} - 1\right) = \frac{k_{tm}q_0m}{Q} - k_{tm}C_0t \quad (9)$$

Table 2

Constant amounts in models of Adams-Bohart, Thomas and Yoon-Nelson in different operational conditions, with the linear regression analysis

Operation conditions			Adam-Bohart model			Thomas model			Yoon-Nelson model		
Z (Cm)	Q (ml/min)	C ₀ (mg/l)	k _{ab} (L/mg*min)	N ₀ (mg/l)	R ²	k _{th}	q ₀ (mg/g)	R ²	k _{Y-N}	τ (min ⁻¹)	R ²
3.5	6	500	1*10 ⁻⁵	22092.8	0.736	2.82*10 ⁻⁵	35004.255	0.901	0.014	29.170	0.901
4.5	6	500	4.8*10 ⁻⁶	38054.8	0.887	1.34*10 ⁻⁵	14366.74	0.952	0.006	16.761	0.952
3.5	8	500	9.2*10 ⁻⁶	23933.71	0.717	3.42*10 ⁻⁵	4659.649	0.911	0.017	2.912	0.911
3.5	10	500	9.6*10 ⁻⁶	25953.73	0.748	4.48*10 ⁻⁵	464.285	0.944	0.022	0.232	0.944
3.5	6	400	1.175*10 ⁻⁵	22418.32	0.847	3.275*10 ⁻⁵	63259.08	0.964	0.013	65.885	0.964
3.5	6	300	3.133*10 ⁻⁵	4078.756	0.934	3.13*10 ⁻⁵	40342.98	0.989	0.0089	44.943	0.989
			R ² _{avg} = 0.811			R ² _{avg} = 0.943			R ² _{avg} = 0.943		

where C_t is the output concentration at any moment, m is adsorbent mass (g) in the column and Q (ml/min) is the inlet flow discharge in the column. k_{Th} is Thomas rate constant (ml/min mg) and q_0 (mg/g) is the maximum amount of the output concentration in the column. k_{Th} and q_0 values are obtained for $\ln\left(\frac{C_0}{C_t} - 1\right)$ curve vs. t (min) [29].

Fig. 7. The experimental and theoretical data of the Thomas model. shows the chart of C_0/C_t according to t (min) shown for all experimental and theoretical data of Thomas model.

The obtained values k_{Th} and q_0 in the column are presented in Table 2. Constant amounts in models of Adams-Bohart, Thomas and Yoon-Nelson in different operational conditions, with the linear regression analysis. The increase of the height and input concentration can be led to decrease k_{Th} , but with increasing the discharge, its value also increased. The q_0 can be decreased by the height and inlet concentration enhancement. The q_0 was firstly increased and then decreased by discharge enhancement. As shown in Table 3, the Thomas model was consistent with mean square error $R^2_{avg} = 0.943$ of experimental data as well as $q_{e,exp}$ and $q_{e,the}$ with Error_{avg} % = ±0.308%.

3.4.3. Yoon-Nelson model

The Yoon-Nelson model is built on the assumption that the rate of decrease in the adsorption probability occurring for each adsorbate molecule is proportional to the probability of adsorbate adsorption and the adsorbate breakthrough probability on the adsorbent [28].

$$\ln\left(\frac{C_t}{C_0 - C_t}\right) = k_{YN}t - \tau k_{YN} \quad (10)$$

where k_{YN} (min⁻¹) and τ (min) are constant amounts in the equation, τ (min) indicated the time that 50% of adsorption process is performed. The equation constant is obtained

$\ln\left(\frac{C_t}{C_0 - C_t}\right)$ by curve vs. t (min) [29]. Fig 8 shows the chart of $C_0/C_0 - C_t$ according to t (min) shown all experimental and theoretical data of Yoon-Nelson model.

The values of K_{YN} in the column decreased while the height increased. This would also increase as the inlet dis-

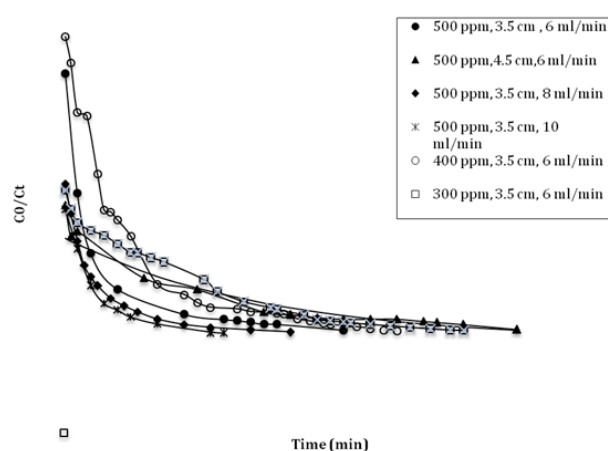


Fig. 7. The experimental and theoretical data of the Thomas model.

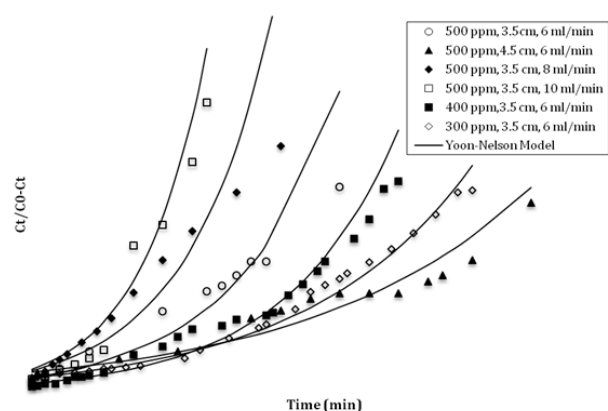


Fig. 8. The experimental and theoretical data of the Yoon-Nelson model.

charge increased. According to this increase, the concentration was firstly increased and then decreased. τ (min⁻¹) decreased while the height of the adsorbent bed, inlet discharge and inlet concentration increased showing by

Table 3
Comparison of the adsorption capacity of theoretical and experimental models of Thomas and Yoon-Nelson models

Operation conditions			Experimental adsorption capacity	Thomas model		Yoon-Nelson model	
Z (Cm)	Q (ml/min)	C ₀ (mg/l)	q _{e,exp} (mg/g)	q _{e,the} (mg/g)	Error%	q _{e,the} (mg/g)	Error%
3.5	6	500	56.061	51.626	7.910	62.257	-11.051
4.5	6	500	75.204	78.613	-4.533	78.613	-4.533
3.5	8	500	54.664	59.414	-8.689	56.629	-3.595
3.5	10	500	50.275	50.562	-0.572	54.886	-9.172
3.5	6	400	71.829	76.78	-6.892	76.78	-6.892
3.5	6	300	75.295	67.069	+10.925	64.541	14.282

doing this process, the column life became shorter. This model based on $R^2_{avg} = 0.943$ is consistent with experimental data. As shown in Table 3, $q_{e,exp}$ and q_e , the with the $Error_{avg} \% = \pm 34.93\%$ are consistent with the Yoon-Nelson model.

Constant values of three kinetic models, Thomas, Yoon-Nelson and Adam-Bohart were calculated for columns data and according to the models, suitable models can be obtained for the column. As shown in Table 2. Constant amounts in models of Adams-Bohart, Thomas and Yoon-Nelson in different operational conditions, with the linear regression analysis, Thomas and Yoon-Nelson models with $R^2_{avg} = 0.943$ and $R^2_{avg} = 0.943$ were fit to the experimental data, respectively, while the Adam-Bohart model with $R^2_{avg} = 0.811$ did not cover the data.

As shown in Table 3, the values of theoretical and experimental data of the adsorption capacity at equilibrium were calculated for Thomas and Yoon-Nelson models and the percentage error of experimental and theoretical values obtained, Thomas and Yoon-Nelson models with $Error_{avg} \% = +10.9\%$ to -8.9% and $Error_{avg} \% = +14.282\%$ to -11.05% have been consistent with experimental results, respectively.

4. Conclusion

In the present study, the sodium alginate/activated carbon/hydroxyapatite hydrogel was synthesized by a sol-gel method, and then used for adsorption of copper ions from aqueous solutions, in constant substrate column. Several experiments were run in order to investigate the effect of the different parameters on the constant substrate column; we found when the column height increased, the inlet flow rate decreased and a decrease in the pollutant inlet concentration can be led to increase the removal percentage of Cu(ii) ion and equilibrium adsorbance. The experimental data were well compatible with Thomas and Yoon-Nelson models ($R^2_{avg} = 0.943$). The percentage error was obtained for adsorbance capacity between the experimental and theoretical values for the Thomas and Yoon-Nelson models 0.308% and 3.493%, respectively. The adsorbent can be regenerated and reused up to 5 cycles using percentage coefficient of adsorbent (D%) 70–82.75%.

Symbols

m (g)	— Amount of adsorbent at the column
V_i (ml)	— Total volume of pollutants entering
Q (cm ³ /min)	— Volumetric flow rate
t_{total} (min)	— Total time of column flow
q_{total} (mg)	— Total adsorption capacity of the column
C_{ad} (mg/L)	— Metal adsorbed concentration
q_e (mg)	— Equilibrium adsorption capacity
W_{total} (mg)	— Total amount of pollutants entering the column
R%	— Percent of the total emitted amount of contaminant in the column
D%	— Desorption %
k_{AB} (L/mg min)	— Constant ratio of adsorption
N_0 (mg/L)	— Saturated concentration
Z (cm)	— Column length
A (cm ²)	— Column sectional area
k_{Th} (ml/min mg)	— Thomas rate constant
q_0 (mg/g)	— Highest output concentration of the column
k_{YN}	— Yoon-Nelson rate constant
τ (min ⁻¹)	— Indicates the time that 50% of adsorption process is done

Acknowledgment

This paper was produced from a MSc Thesis conducted at the Department of Chemical Engineering, Omidiyeh and Mahshahr branch, Islamic Azad University, Omidiyeh and Mahshahr, Iran.

References

- [1] Y. Yan, X. Dong, X. Sun, X. Sun, J. Li, J. Shen, W. Han, X. Liu, L. Wang, Conversion of waste FGD gypsum into hydroxyapatite for removal of Pb²⁺ and Cd²⁺ from wastewater, J. Colloid. Interf. Sci., 429 (2014) 68–76.
- [2] X.-J. Ju, S.-B. Zhang, M.-Y. Zhou, R. Xie, L. Yang, L.-Y. Chu, Novel heavy-metal adsorption material: ion-recognition P(NI-PAM-co-BCAm) hydrogels for removal of lead(II) ions, J. Hazard. Mater., 167 (2009) 114–118.
- [3] T. Lu, T. Xiang, X.-L. Huang, Ch. Li, W.-F. Zhao, Q. Zhang, Ch.-Sh. Zhao, Post-crosslinking towards stimuli-responsive sodium alginate beads for the removal of dye and heavy metals, Carbohydr. Polym., 133 (2015) 587–595.

- [4] B. Hui, Y. Zhang, L. Ye, Structure of PVA/gelatin hydrogel beads and adsorption mechanism for advanced Pb(II) removal, *J. Ind. Eng. Chem.*, 21 (2015) 868–876.
- [5] Y. Shang, X. Yu, Screening of algae material as a filter for heavy metals in drinking water, *Algal Res.*, 12 (2015) 258–261.
- [6] I. Mobasherpour, E. Salahi, M. Pazouki, Removal of nickel (II) from aqueous solutions by using nano-crystalline calcium hydroxyapatite, *J. Saudi Chem. Soc.*, 15 (2011) 105–112.
- [7] L. Wang, J. Zhang, A. Wang, Fast removal of methylene blue from aqueous solution by adsorption onto chitosan-g-poly (acrylic acid)/attapulgitite composite, *Desalination*, 266 (2011) 33–39.
- [8] S. Zhao, F. Zhou, L. Li, Cao, D. Zuo, H. Liu, Removal of anionic dyes from aqueous solutions by adsorption of chitosan-based semi-IPN hydrogel composites, *Compos. Part. B. Eng. J.*, 43 (2012) 1570–1578.
- [9] E. Ramirez, S.G. Burillo, C. Barrera-Diaz, G. Roa, B. Bilyeu, Use of pH-sensitive polymer hydrogels in lead removal from aqueous solution, *J. Hazard. Mater.*, 192 (2011) 432–439.
- [10] A. Koteja, J. Matusik, Di- and triethanolamine grafted kaolinites of different structural order as adsorbents of heavy metals, *J. Colloid. Interf. Sci.*, 455 (2015) 83–92.
- [11] O. Ozay, S. Ekici, Y. Baran, N. Aktas, N. Sahiner, Removal of toxic metal ions with magnetic hydrogels, *Water. Res.*, 43 (2009) 4403–4411.
- [12] G. Zhou, Ch. Liu, Y. Tang, Sh. Luo, Z. Zeng, Y. Liu, R. Xu, L. Chu, Sponge-like polysiloxane-curveene oxide gel as a highly efficient and renewable adsorbent for lead and cadmium metals removal from wastewater, *Chem. Eng. J.*, 280 (2015) 275–282.
- [13] Y. Zheng, Y. Liu, A. Wang, Fast removal of ammonium ion using a hydrogel optimized with response surface methodology, *Chem. Eng. J.*, 171 (2011) 1201–1208.
- [14] A. Zamani, D. Henriksson, M.J. Taherzadeh, A new foaming technique for production of superadsorbents from carboxymethyl Chitosan, *Carbohydr. Polym.*, 80 (2010) 1091–1101.
- [15] X.-N. Shi, W.-B. Wang, A.-Q. Wang, Effect of surfactant on porosity and swelling behaviors of guar gum-g-polyb (sodium acrylate-co-styrene)/attapulgitite superadsorbent hydrogels, *Colloids Surf. B Biointerfaces*, 88 (2011) 279–286.
- [16] M.G. Dekamin, S.Z. Peyman, Z. Karimi, Sh. Javanshir, M.R. Naimi-Jamal, M. Barikani, Sodium alginate, An efficient biopolymeric catalyst for green synthesis of 2-amino-4H-pyran derivatives, *Int. J. Biol. Macromolec.*, 87 (2016) 172–179.
- [17] Lee Kuen Yong, J. Mooney David, Alginate: properties and biomedical applications, *Prog. Polym. Sci.*, 37 (2012) 106–126.
- [18] Ch. Jiao, J. Xiong, J. Tao, S. Xu, D. Zhang, H. Lin, Y. Chen, Sodium alginate/graphene oxide aerogel with enhanced strength-toughness and its heavy metal adsorption study, *Int. J. Biol. Macromolec.*, 83 (2016) 133–141.
- [19] A. Bhatnagar, W. Hogland, M. Marques, M. Sillanpaa, An overview of the modification methods of activated carbon for its water treatment applications, *Chem. Eng. J.*, 219 (2013) 499–511.
- [20] M.H. Givianrad, M. Rabani, M. Saber-Tehrani, P. Aberoomand-Azar, M. Hosseini Sabzevari, Preparation and characterization of nanocomposite, silica aerogel, activated carbon and its adsorption properties for Cd (II) ions from aqueous solution, *J. Saudi Chem. Soc.*, 17 (2013) 329–335.
- [21] M. Jain, V.K. Garg, K. Kadirvelu, Cadmium(II) sorption and desorption in a fixed bed column using sunflower waste carbon calcium-alginate beads, *Bioresour Technol.*, 129 (2013) 242–248.
- [22] M. Jain, V.K. Garg, K. Kadirvelu, Mika Sillanpaa, Combined effect of sunflower stem carbon-calcium alginate beads for the removal and recovery of chromium from contaminated water in column mode, *Ind. Eng. Chem. Res.*, 54 (2015) 1419–1425.
- [23] J. Moreno-Pérez, A. Bonilla-Petriciolet, C.K. Rojas-Mayorga, D.I. Mendoza-Castillo, M. Mascia, M. Errico, Adsorption of zinc ions on bone char using helical coil-packed bed columns and its mass transfer modeling, *Desal. Water Treat.*, 51 (2016) 24200–24209.
- [24] A. Garba, N. Sh. Nasri, H. Basri, I. Razali, A.M. Zulkifli, U.D. Hamza, M. Jibril, Adsorptive removal of phenol from aqueous solution on a modified palm shell-based carbon: fixed-bed adsorption studies, *Desal. Water Treat.*, 57 (2016) 29488–29499.
- [25] Y. Zhuang, F. Yu, J. Chen, J. Ma, Batch and column adsorption of methylene blue by curveene/alginate nanocomposite Comparison of single-network and double-network hydrogels, *J.E.C.E.*, 4 (2016) 147–156.
- [26] G.J. Copello, A.M. Mebert, M. Raineri, M.P. Pesenti, L.E. Diaz, Removal of dyes from water using chitosan hydrogel/SiO₂ and chitin hydrogel/SiO₂ hybrid materials obtained by the sol-gel method, *J. Hazard. Mater.*, 186 (2011) 932–939.
- [27] M.A. Ahmed, M.F. Abdel-Messih, Structural and nano-composite features of TiO₂-Al₂O₃ powders prepared by sol-gel method, *J. Alloy Compd.*, 509 (2011) 2154–2159.
- [28] M. Foroughi-dahr, M. Esmaili, H. Abolghasemi, A. Shojamoradi, E. Sadeghi Pouya, Continuous adsorption study of congo red using tea waste in a fixed-bed column, *Desal. Water Treat.*, 57 (2016) 8437–8446.
- [29] M. Mansour Lakouraj, F. Mojerlou, E. Nazarzadeh Zare, Nanogel and super paramagnetic nanocomposite based on sodium alginate for sorption of heavy metal ions, *Carbohydr. Polym.*, 106 (2014) 34–41.
- [30] A.F. Elsheikh, A. Umi Kalthom, Z. Ramli, Removal of humic acid from water by adsorption onto dodecyltrimethylammonium bromide-modified zeolite in a fixed bed reactor, *Desal. Water Treat.*, 57 (2016) 8302–8318.